

Supporting Information

A phosphite based layered framework as a novel positive electrode material for Na-ion Batteries

A. Shahul Hameed,^{ab} Mirai Ohara,^a Kei Kubota,^{ab} and Shinichi Komaba^{*ab}

^aDepartment of Applied Chemistry, Tokyo University of Science, Tokyo 162-8601, Japan.

^bESICB, Kyoto University, 1-30 Goryo-Ohara, Nishikyo-ku, Kyoto 615-8245, Japan

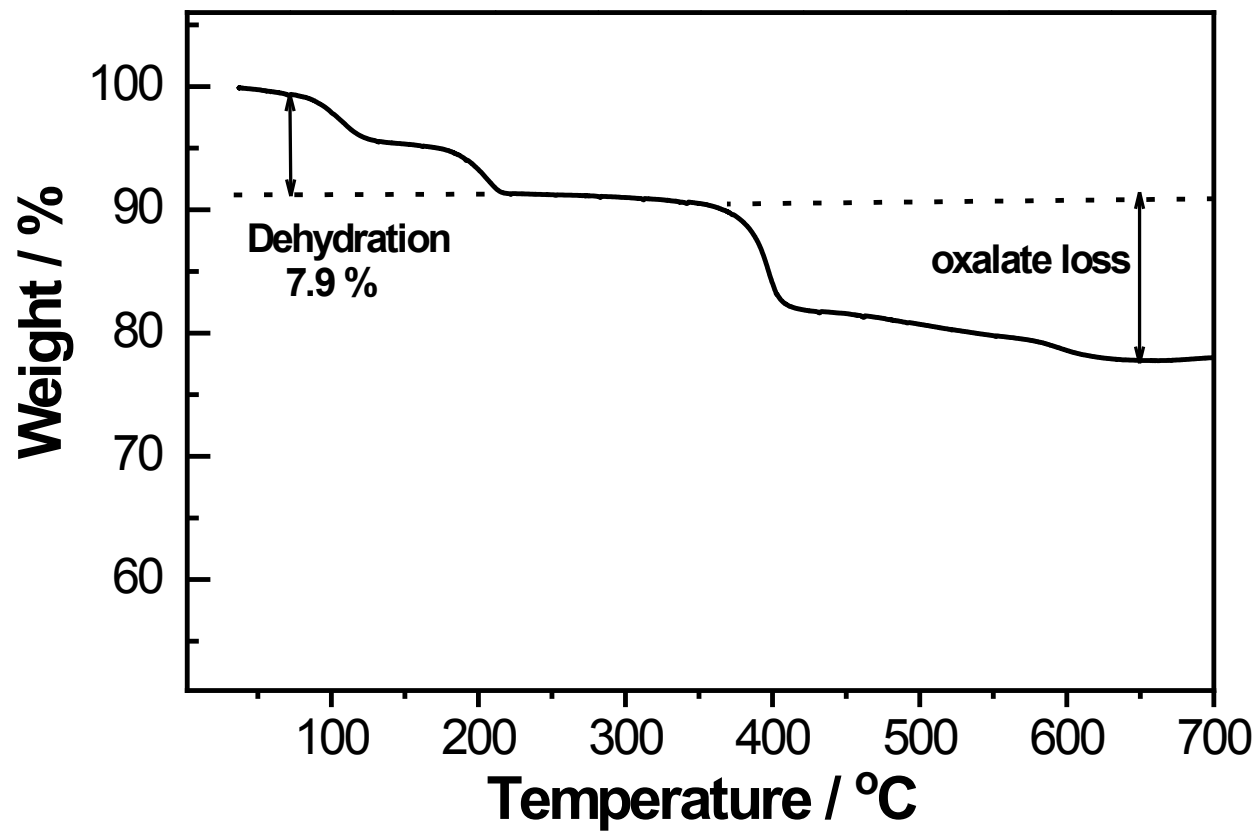


Fig. S1: TGA of p-NVPox in nitrogen atmosphere at a scan rate of 5 °C min⁻¹

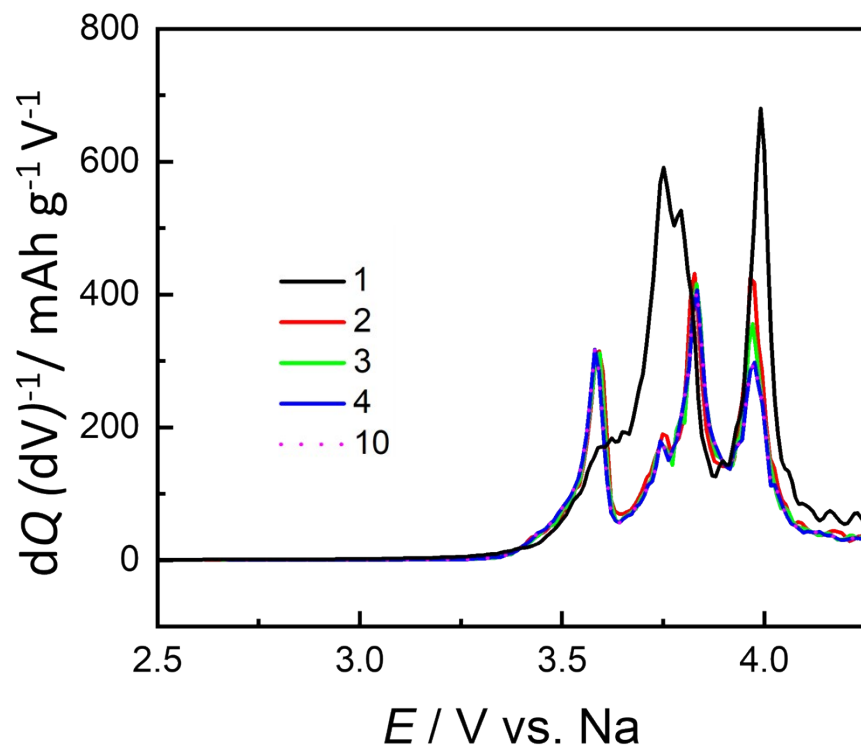
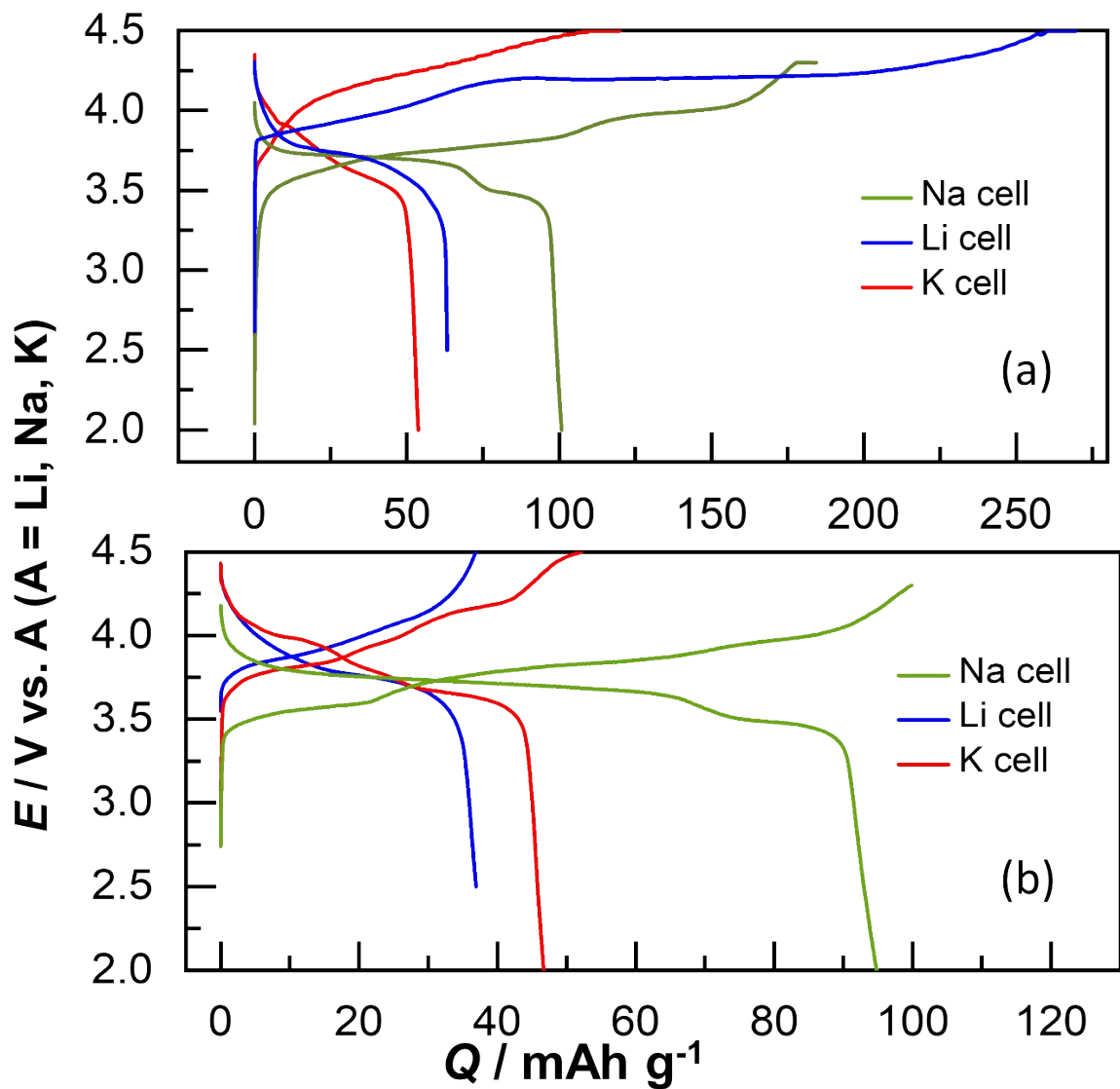


Fig. S2: The dQ/dV plots of p-NVPox (charge curves) for selected cycles



8

Fig. S3: Comparison of charge-discharge profiles of p-NVPox in Li-, Na- and K-half cells at 0.1 C for (a) 1st cycle, and (b) 10th cycle.

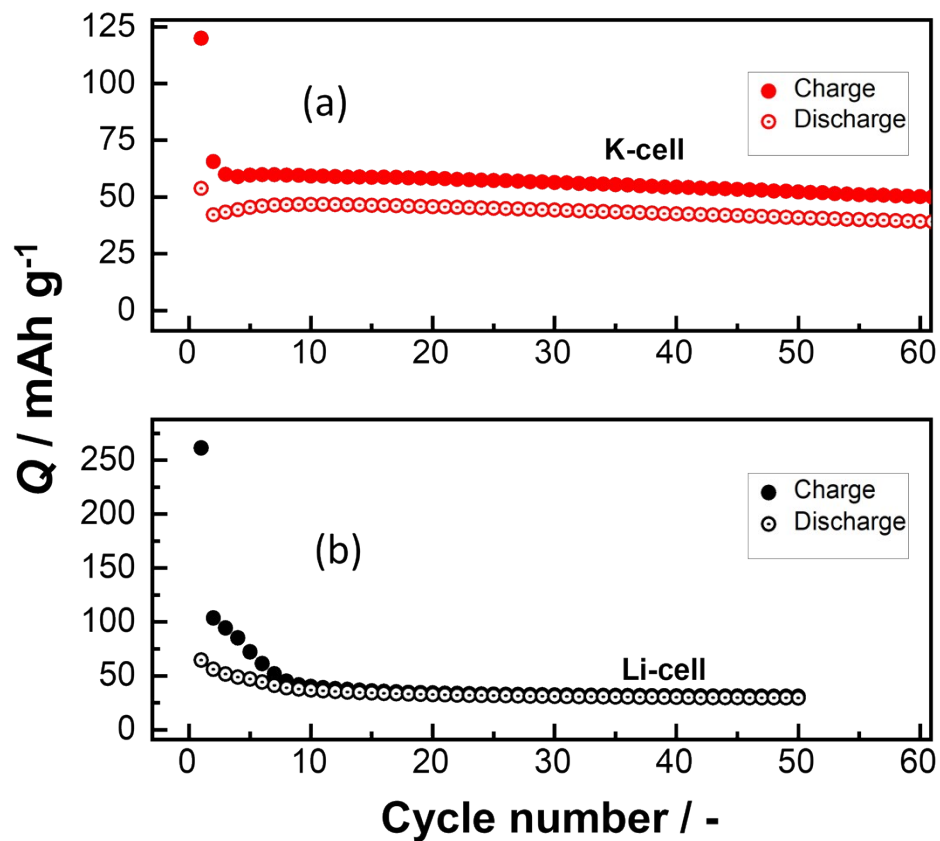


Fig. S4: Capacity retention plots of p-NVPox at 0.1 C in (a) K- half cell and (b) Li-half cell.

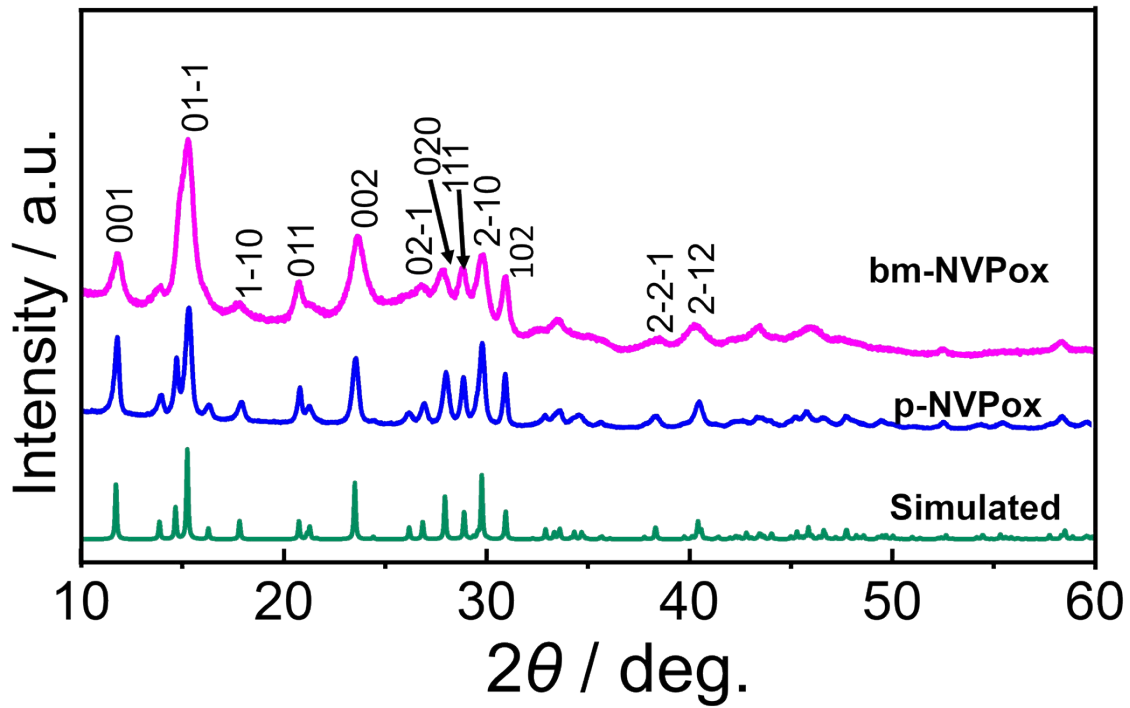


Fig. S5: Comparison of XRD patterns of bm-NVPox and p-NVPox with the simulated pattern of $\text{Na}_2[(\text{VOHPO}_3)_2(\text{C}_2\text{O}_4)] \cdot 2\text{H}_2\text{O}$

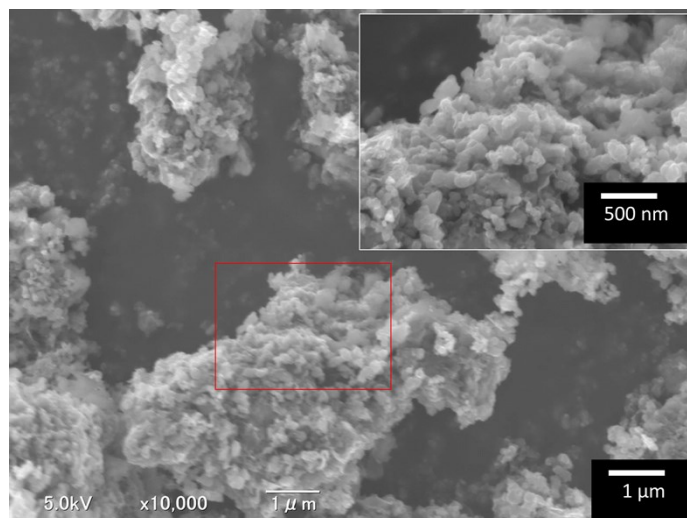


Fig. S6: SEM micrograph of bm-NVPox. The inset shows a higher magnification image (x30,000) of the selected area.

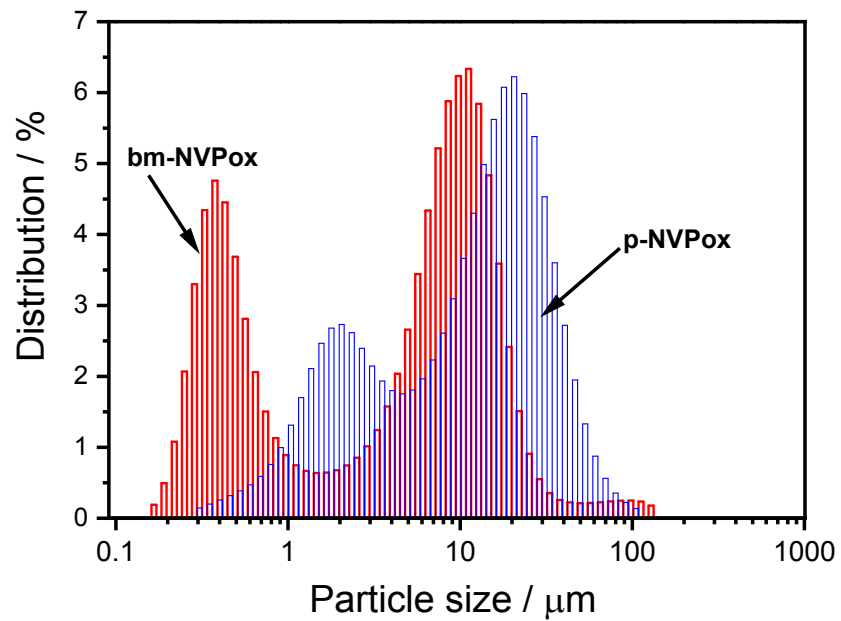


Fig. S7: Comparison of particle size of ball milled NVPOx and the pristine sample.

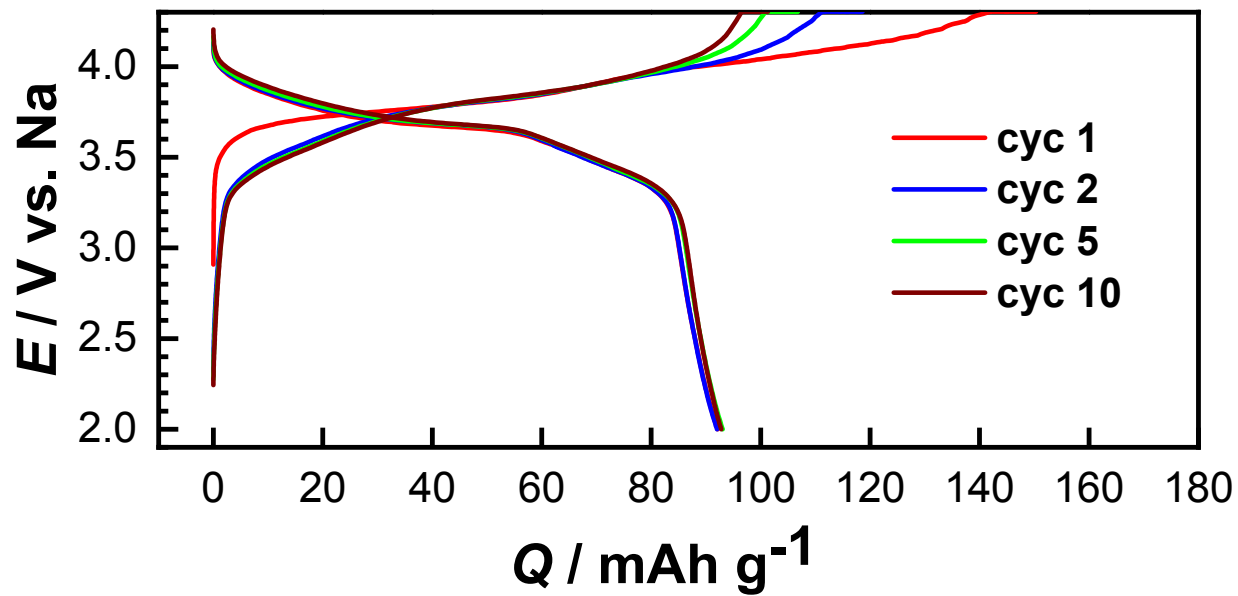


Fig. S8: Charge-discharge profiles of bm-NVPox for 10 cycles at 0.1 C current rate in the potential range of 2.0-4.3 V.

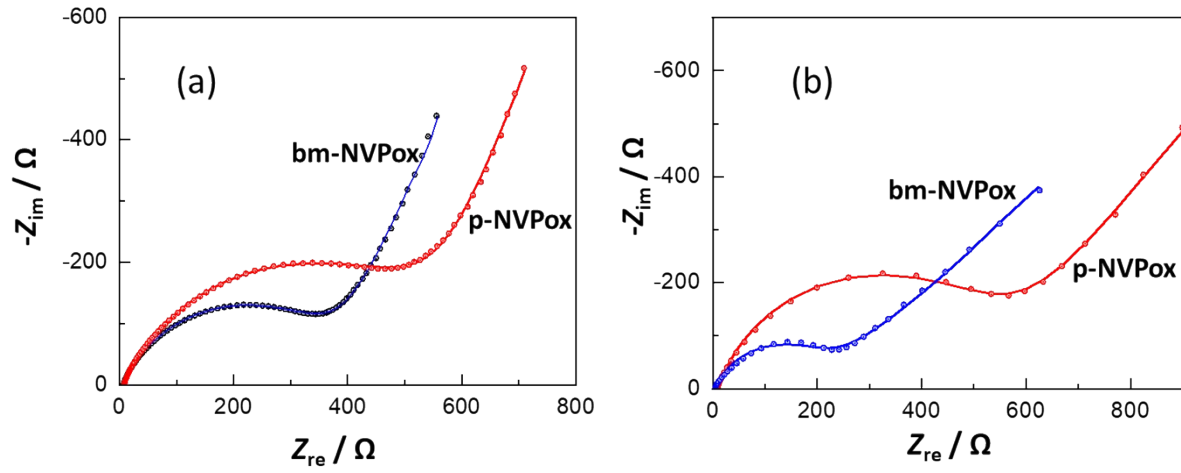


Fig. S9: Nyquist plots of p-NVPox and bm-NVPox during first cycle: (a) charged state (4.3V) and (b) discharged state (2.0 V). The circles represent experimental values and the solid line represent fitted results.

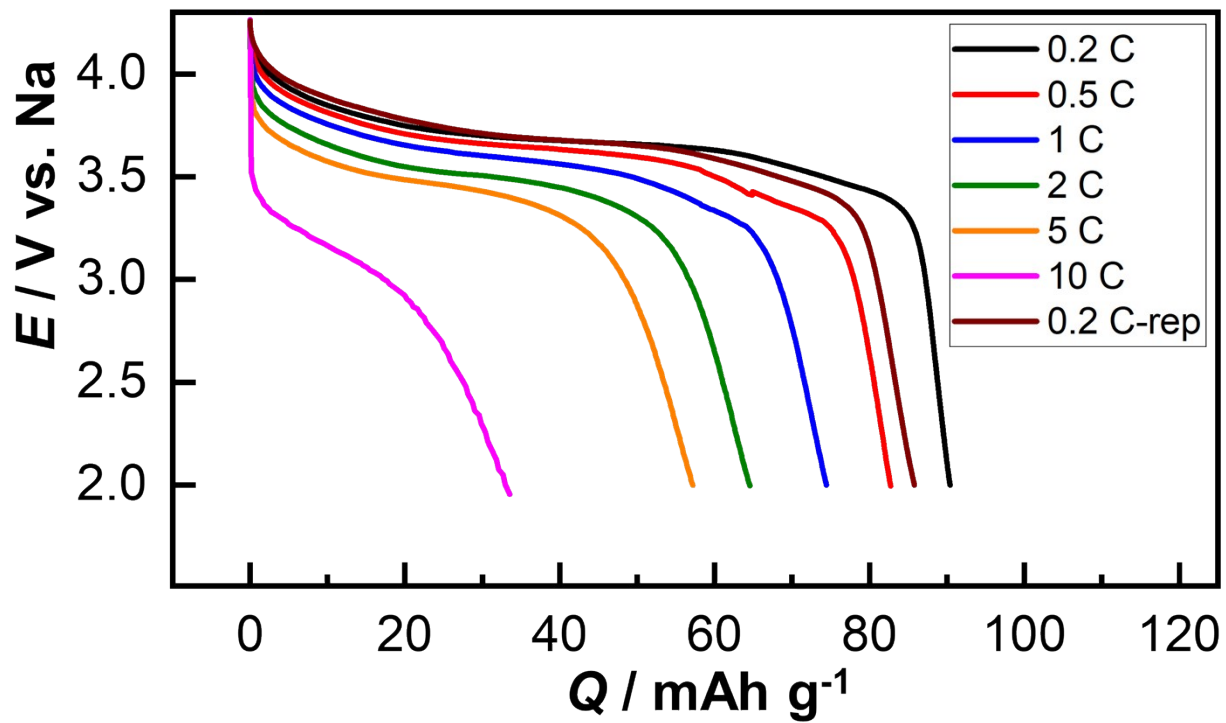


Fig. S10: Comparison of discharge profiles of p-NVPox at different current rates.

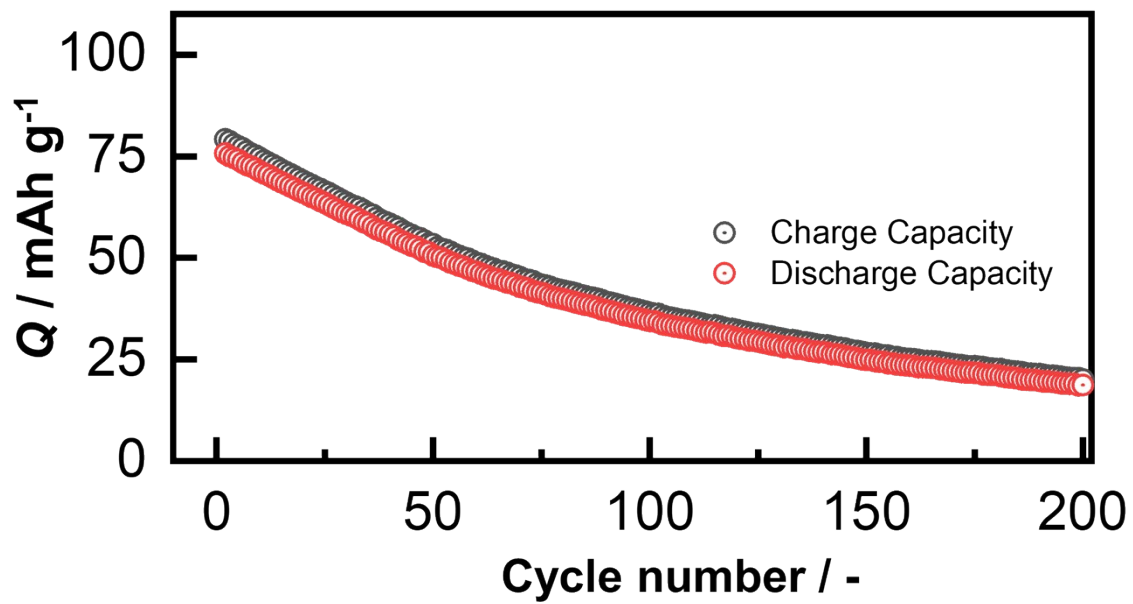


Fig. S11: Long term cycling of p-NVPox at 2 C rate showing charge and discharge capacities for 200 cycles.

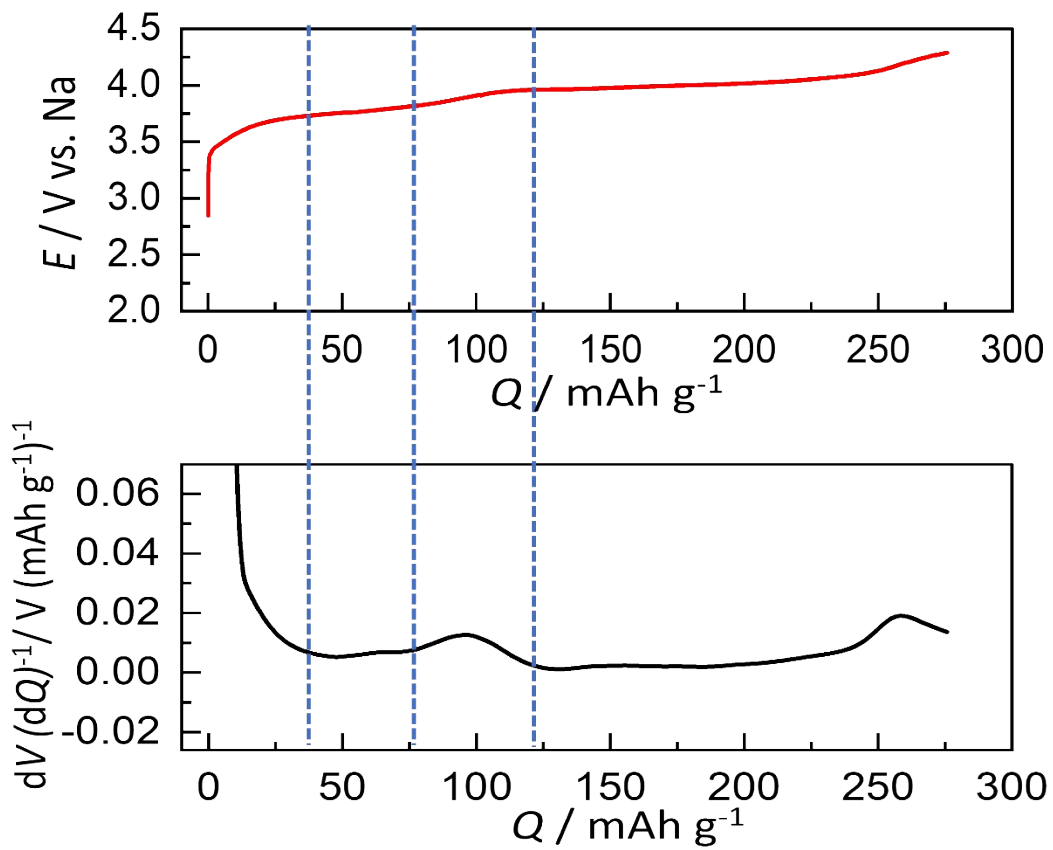


Fig. S12: Differential voltage analysis (dV/dQ) of the first charge curve of p-NVPox during the operando XRD measurement.

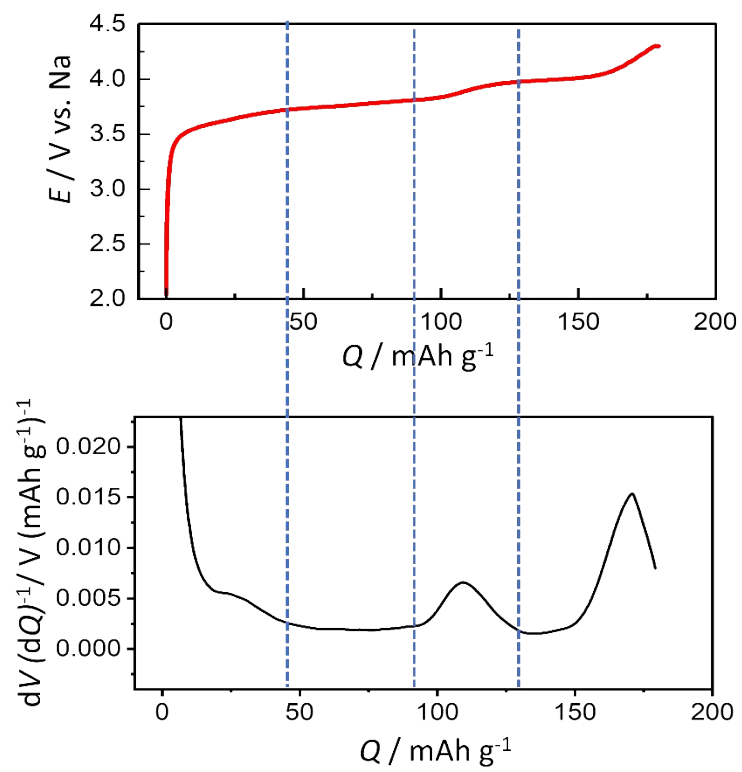


Fig. S13: Differential voltage analysis (dV/dQ) of the first charge curve of p-NVPox in a coin cell.

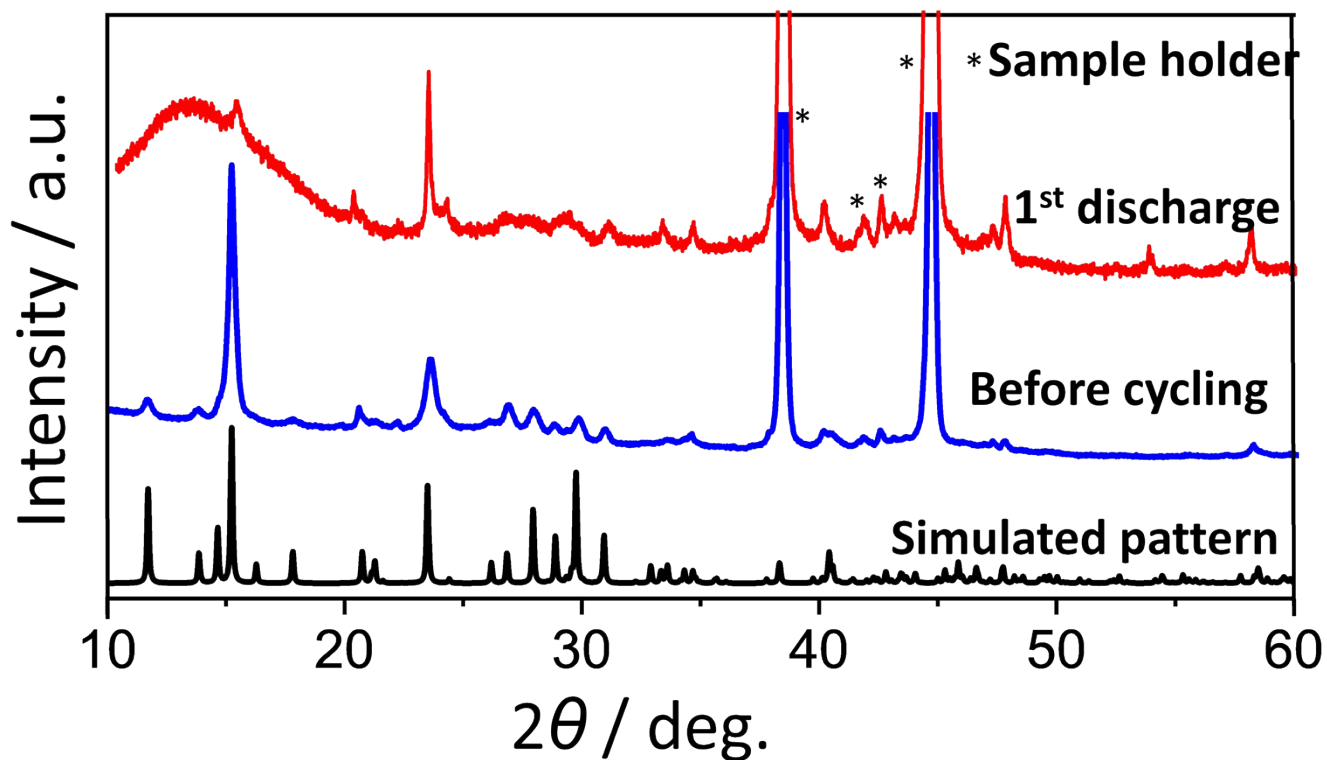


Fig. S14: XRD patterns of p-NVPox electrode before cycling and at the end of first discharge compared with the simulated pattern of NVPOx.

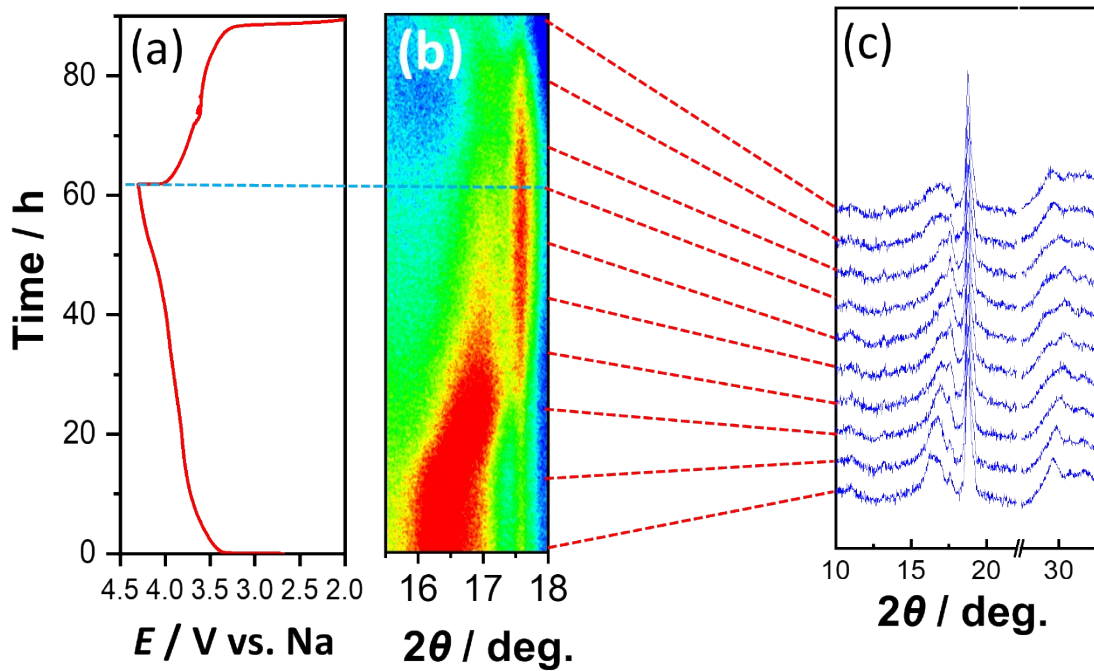


Fig. S15: Structural evolution during second Na extraction/insertion: a) Charge-discharge profile during the operando XRD measurement, (b) contour maps of operando XRD for selected 2θ regions and c) XRD patterns at selected SOC.

Synthesis of c-NaTi₂(PO₄)₃

0.01 M Ti(OBu)₄ was added to 40 mL of 30% H₂O₂ with constant stirring and 15 mL of 28% NH₄OH was added and stirred. Then stoichiometric amounts of citric acid, (NH₄)₂HPO₄ and Na₂CO₃ were added, followed by ethylene glycol. After stirring for few hours, the resulting solution was dried at 80 °C in air under constant stirring. The powder was calcined at 350 °C for 3h in air and then at 700 °C for 12h in air to obtain the white NaTi₂(PO₄)₃.(NTP) powder. The carbon coating was carried out by hydrothermal treatment of NTP(200 mg) with sucrose (500 mg) at 180 °C for 6h, followed by calcination at 800 °C for 1h in Ar.

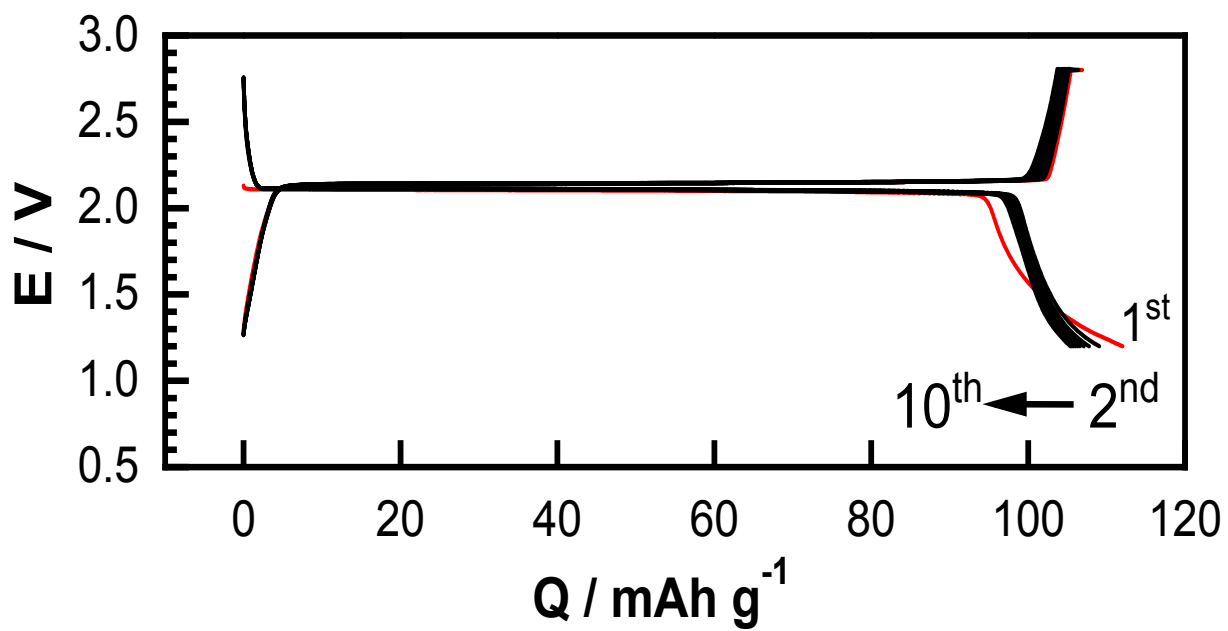


Fig. S16: Charge-discharge profiles of a $\text{NaTi}_2(\text{PO}_4)_3$ (NTP) half-cells

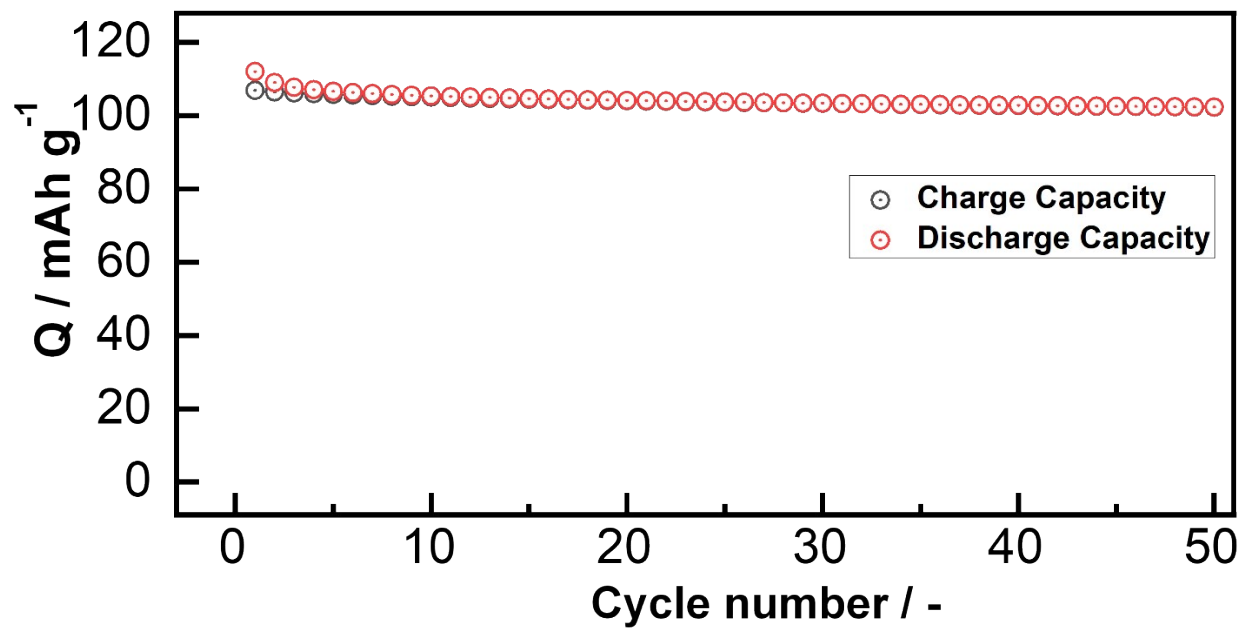


Fig. S17: Capacity retention plots of a NaTi₂(PO₄)₃ (NTP) half-cell.